Reactions of Laser-Ablated Molybdenum and Tungsten Atoms with Nitric Oxide. Infrared Spectra of the MN, NMO, and M-η^1-$(NO)_x$ (x = 1, 2, 3, 4) Molecules and $(NO)_2^+$ and $(NO)_2^-$ Ions in Solid Argon

Lester Andrews* and Mingfei Zhou

Department of Chemistry, University of Virginia, Charlottesville, Virginia 22901

Received: January 27, 1999; In Final Form: March 16, 1999

Laser-ablated Mo and W atoms react with NO to give primarily the nitride−oxide insertion products NMoO and NWO, but weak MoN and WN absorptions are also observed. The NMoO and NWO molecules are identified from isotopic substitution (^{n}Mo, ^{15}N, ^{18}O) and density functional theory (DFT) calculations. The M−N and M−O stretching frequencies of the ^{2}A′ state NMoO and NWO molecules are predicted by DFT (scale factors 0.936 ± 0.004 and 0.966 ± 0.005, respectively), but more importantly, the isotopic shifts (and normal modes) are well-described by DFT isotopic frequencies. The higher energy MoNO isomer is observed, but WNO and the M-η^2-NO complexes are not found. The M-(η^1-NO)$_x$ (x = 2, 3, 4) complexes are observed: mixed isotopic splittings indicate that $Mo(NO)_4$ is tetrahedral, like $Cr(NO)_4$, but the spectra show that $W(NO)_4$ is distorted to C_{2v} symmetry. In addition, a weak 3643.5 cm^{-1} combination band and strong 1589.3 cm^{-1} fundamental for $(NO)_2^+$ and the strong fundamentals for *cis*- and *trans*-$(NO)_2^-$ were observed.

1. Introduction

Small molecules bound to metal clusters are models for studies of chemisorption, catalysis, and corrosion. Atom−molecule complexes are the first step in the formation of such ligand-bound clusters.[1,2] Previous work in this laboratory has shown that Cr atoms form the four expected nitrosyls Cr-[η^1-NO]$_{1-4}$ and the novel NCrO insertion product, a nitride and oxide molecule with parallels to CrO_2 and CrN_2.[3−5] An analogous vertical matrix infrared investigation of laser-ablated V, Nb, and Ta atom reactions with NO has revealed the NMO insertion product and M-[η^1-NO]$_{1-3}$ complexes.[6,7] It follows that laser-ablated Mo and W atoms will form products analogous with Cr, and this investigation will be reported here. Since Cr-[η^1-NO]$_4$ is the only stable transition metal nitrosyl,[8,9] the analogous Mo and W tetranitrosyl species are expected to be the dominant products. The bulk oxides and nitrides of molybdenum and tungsten have important catalytic and electrical properties,[10−20] but little is known about mixed nitride−oxides. Hence, the metal reactions with NO provide a controlled means for preparing mixed nitride−oxides.

2. Experimental Section

The experiments of laser ablation and FTIR matrix investigation have been described previously.[21,22] The 1064 nm Nd:YAG laser beam (Spectra Physics, DCR-11) was focused by a 10 cm focal length lens onto the rotating metal target (Mo, Goodfellow, 99% and W, Johnson-Matthey, 99.98%). The laser repetition rate is 10 Hz with a pulse width of 10 ns. Different laser powers ranging from 20 to 40 mJ/pulse at the sample were used in the experiments. The ablated metal atoms were co-deposited with 0.3% NO/Ar gas onto the 10 K CsI window at a rate of 2−4 mmol/h for 1−2 h. Different isotopic NO samples (^{14}N^{16}O, Matheson; ^{15}N^{16}O, Isomet, 99%; ^{15}N^{18}O, Isotec, 99%) and selected mixtures were used. FTIR spectra were recorded with 0.5 cm^{-1} resolution and 0.1 cm^{-1} accuracy on a Nicolet 750 using a HgCdTe detector. Matrix samples were annealed at different temperatures, and selected samples were subjected to broad-band photolysis by a medium-pressure mercury arc lamp (Phillips, 175W) with globe removed.

3. Results

Infrared spectra of laser-ablated Mo and W atom reaction products with NO are shown in Figures 1−6, and the product absorptions are listed in Tables 1 and 2. Absorptions common to these experiments, namely $(NO)_2$, NO_2, N_2O, NO_2^-, $(NO)_2^-$, and $(NO)_2^+$, have been reported in the V and Cr investigations.[3,6,23−28] An unusually high yield of $(NO)_2^+$ was observed here. Annealing and photolysis studies were done to group product bands and characterize the absorbing species.

Experiments were done with ^{15}N^{16}O and ^{15}N^{18}O samples and the same behavior was observed. Isotopic frequencies are also listed in the tables. Similar experiments with 50% ^{14}N^{16}O + 50% ^{15}N^{16}O mixtures gave diagnostic multiplets, which will be discussed below to characterize the several product species.

4. Calculations

Density functional theory (DFT) calculations using the Gaussian 94 program[29] were employed to calculate structure and frequencies for the MNO isomers. The BP86 functional, D95* basis set for nitrogen and oxygen atoms, and Los Alamos ECP plus DZ basis set for metal atoms were used for all calculations.[30−32] These calculations are considered to be a first-order approximation and a guide for vibrational assignments. For both MoNO and WNO isomers, the insertion product NMoO and NWO molecules are calculated to be much more stable than other isomers. The side-bonded M[NO] and nitrosyl MNO isomers are about 30−60 kcal/mol higher in energy than the corresponding NMO insertion products. Tables 3 and 4 summarize the calculated parameters.

5. Discussion

The new product absorptions will be identified and assigned on the basis of isotopic substitution and DFT isotopic frequency calculations.

10.1021/jp990328i CCC: $18.00
Published on Web 05/06/1999

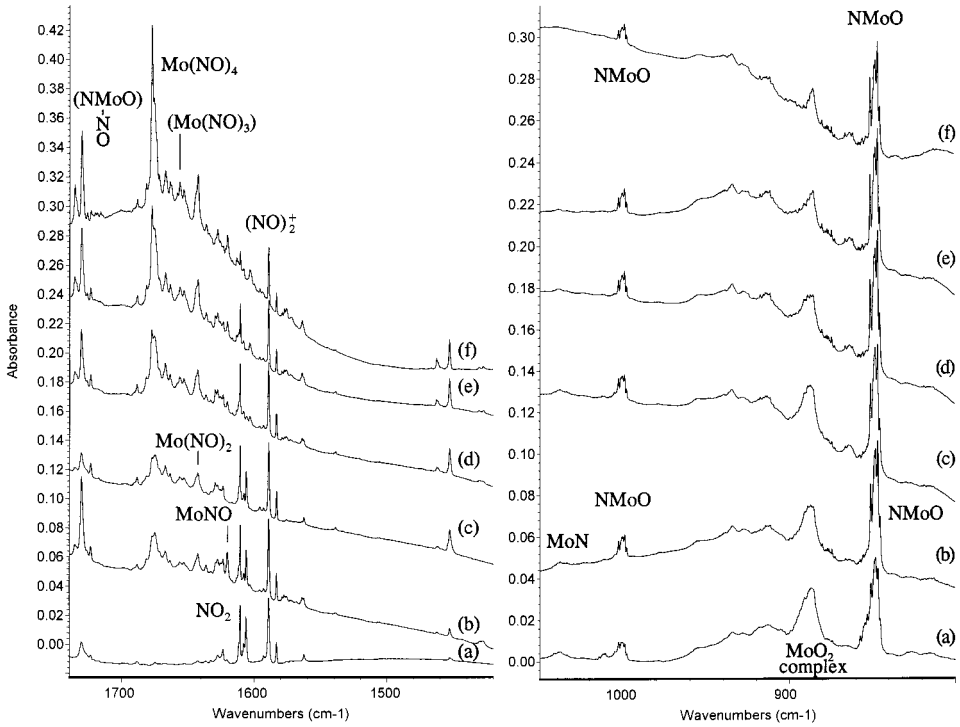

Figure 1. Infrared spectra for laser-ablated Mo atoms co-deposited at 10 K with 0.3% NO in argon: (a) sample deposited for 1 h; (b) sample after annealing to 25 K; (c) sample after broad-band photolysis for 30 min; (d) sample after annealing to 30 K; (e) sample after annealing to 35 K; (f) sample after annealing to 40 K.

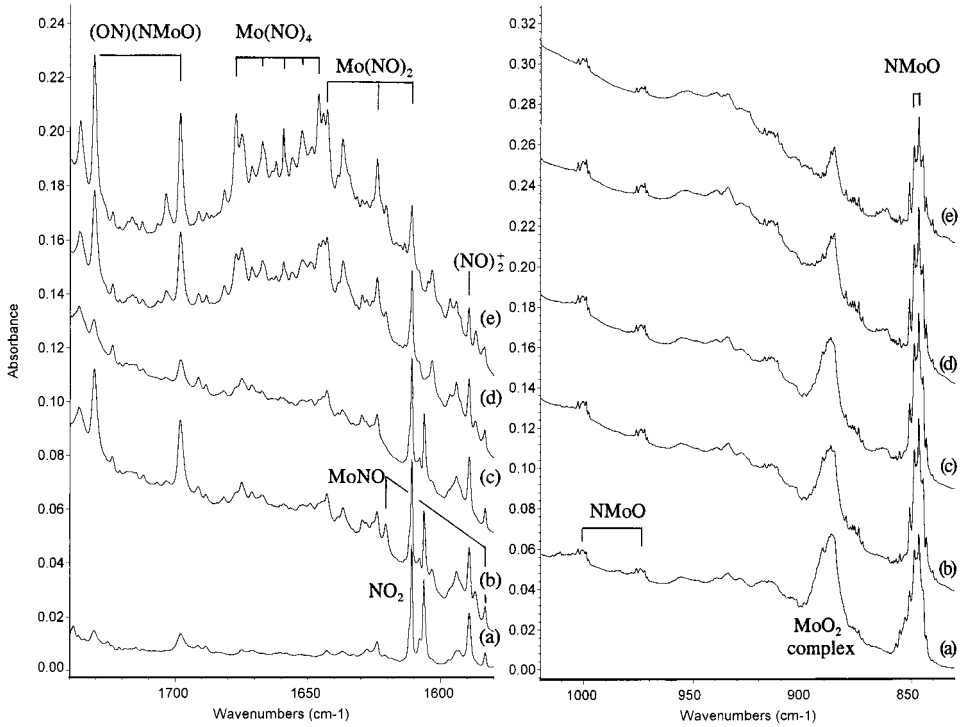

Figure 2. Infrared spectra for laser-ablated Mo atoms co-deposited at 10 K with 0.3% (^{14}NO + ^{15}NO) in argon: (a) sample deposited for 1 h; (b) sample after annealing to 25 K; (c) sample after broad-band photolysis for 30 min; (d) sample after annealing to 30 K; (e) sample after annealing to 40 K.

NMoO. Following the example of NCrO, the NMoO insertion product is characterized by two bond-stretching modes, which are almost pure Mo−N and Mo−O stretching coordinates.[3] First, the structured bands at 1000 and 845 cm^{-1} clearly involve one NO molecule (i.e., one N and one O atom) as the mixed ^{14}NO + ^{15}NO isotopic spectrum gives the sum of pure ^{14}NO and pure ^{15}NO spectra, although the nitrogen 14−15 shift is much larger (26 cm^{-1}) for the upper band (mostly Mo−N stretching) than for the lower band (2 cm^{-1}) (Figures 1 and 2). Second, the resolution of natural molybdenum isotopic splittings for both the upper band at 1002.8, 1000.8, 1000.2, 999.1, and 997.9 cm^{-1} and the lower band at 850.9, 848.5, 847.9, 846.5, and 845.2 cm^{-1} (Figure 3) with absorbances appropriate for the distribution of natural molybdenum isotopes 92 (15.84%), 94 (9.04%), 95

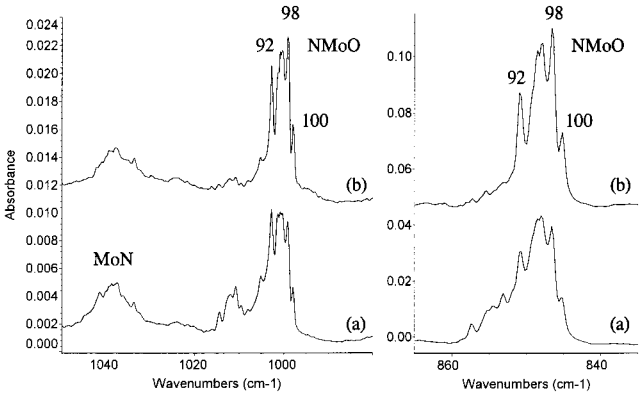

Figure 3. Expanded infrared spectra in the 1050−980 and 870−830 cm^{-1} regions for laser-ablated Mo atoms co-deposited with 0.3% NO: (a) sample deposited for 1 h; (b) sample after annealing to 25 K.

(15.72%), 96 (16.53%), 97 (9.46%), 98 (23.78%), and 100 (9.63%) for the five major isotopic assignments listed in Table 1 clearly shows that one Mo atom is involved in this molecule.

The 999.1 cm^{-1} band for $N^{98}MoO$ shifts to 972.4 cm^{-1} with ^{15}NO, giving the 14/15 ratio 1.027 43, which is slightly smaller than the harmonic ^{98}MoN value (1.030 51) owing to the small oxygen involvement as noted by the 4.4 cm^{-1} shift with $^{15}N^{18}O$. On the other hand, the 846.5 cm^{-1} band for $N^{98}MoO$ shifts only 2.0 cm^{-1} with ^{15}NO and to 807.4 cm^{-1} with $^{15}N^{18}O$, giving a $^{15}N^{16}O/^{15}N^{18}O$ ratio of 1.045 95, which is also slightly smaller than the harmonic ^{98}MoO value (1.051 58) due to the minor nitrogen involvement. The $N^{92}MoO/N^{98}MoO$ ratio for the upper band (1.002 70) is slightly smaller than the harmonic MoN value (1.004 08) and this same isotopic ratio for the lower band (1.005 20) is slightly larger than the harmonic MoO value (1.004 60).

The assignments to NMoO made on the basis of the above isotopic shifts are confirmed by the BP86/D95*/LanL2DZ calculations, which predict modes at 1054.0 and 907.6 cm^{-1} with 44:123 relative intensity for $^2A'$ NMoO. The calculated frequencies must be scaled by 0.940 and 0.933 to fit the observed values, which are slightly lower than other scale factors for these basis sets,[33] but the relative band absorbance matches the calculated relative intensity. Of more importance, the normal modes also agree very well on the basis of the isotopic shifts. The upper band is calculated to shift −29.5 cm^{-1} with ^{15}NO and −2.5 cm^{-1} with $^{15}N^{18}O$, and the observed shifts (^{98}Mo) are −26.7 and −4.4 cm^{-1}; the lower band is calculated to shift −1.3 cm^{-1} with ^{15}NO and −41.9 cm^{-1} with $^{15}N^{18}O$, and the observed shifts are −2.0 and −37.1 cm^{-1}.

It is interesting to compare the 991.1 and 846.5 cm^{-1} stretching frequencies for $N^{98}MoO$ with the observations for $^{98}MoO_2$ (939, 885 cm^{-1})[34] and $^{98}MoN_2$ (975, 861 cm^{-1}).[35] The average stretching frequencies for $^{98}MoO_2$ (912 cm^{-1}) and $^{98}MoN_2$ (918 cm^{-1}) are between the $N^{98}MoO$ values and, in fact, almost agree with the average $N^{98}MoO$ value (919 cm^{-1}). The NMoO molecule is a true nitride *and* oxide with bonding comparable to the molybdenum dioxide and dinitride molecules.

NWO. An analogous case can be made for NWO. The two sharp 1016.3 and 907.3 cm^{-1} bands track together on annealing, and isotopic shifts show almost pure W−N and W−O stretching modes, respectively (Figure 4). The $^{14}N^{16}O/^{15}N^{16}O$ ratio for the upper band is slightly less than the WN value and the $^{15}N^{18}O$ shift is small (−7.1 cm^{-1}), whereas the reverse relationship is found for the lower band: namely, the $^{15}N^{16}O$ shift is small (−4.1 cm^{-1}) and the $^{15}N^{16}O/^{15}N^{18}O$ ratio is slightly less than the WO value (Table 2). The mixed isotopic experiments ^{14}NO + ^{15}NO and $^{15}N^{16}O$ + $^{15}N^{18}O$ (Figure 5) show doublets for these bands without mixed isotopic components, which indicates that a single NO molecule reacts to make the NWO product.

The identification of two stretching modes for NWO from isotopic shifts is confirmed by the DFT/BP86 calculations, which predict bands at 1057.0 and 934.3 cm^{-1} with 20:91 relative intensity for $^2A'$ bent NWO. The calculated frequencies must be scaled by 0.961 and 0.971 to fit the observed values and the

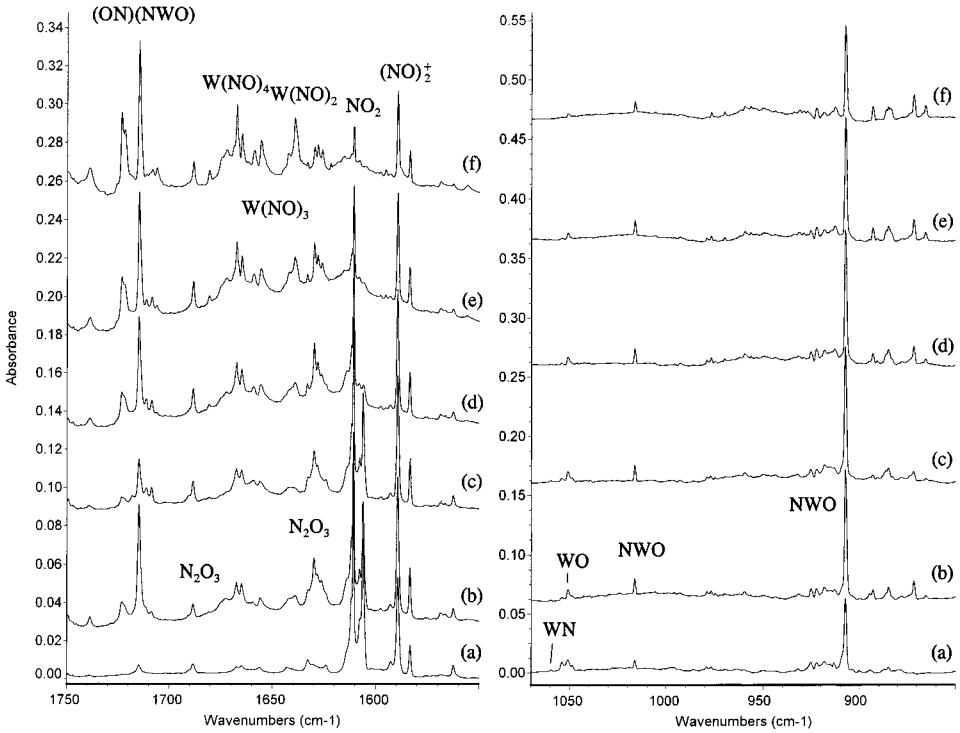

Figure 4. Infrared spectra for laser-ablated W atoms co-deposited at 10 K with 0.3% NO in argon: (a) sample deposited for 1 h; (b) sample after annealing to 25 K; (c) sample after broad-band photolysis for 30 min; (d) sample after annealing to 30 K; (e) sample after annealing to 35 K; (f) sample after annealing to 40 K.

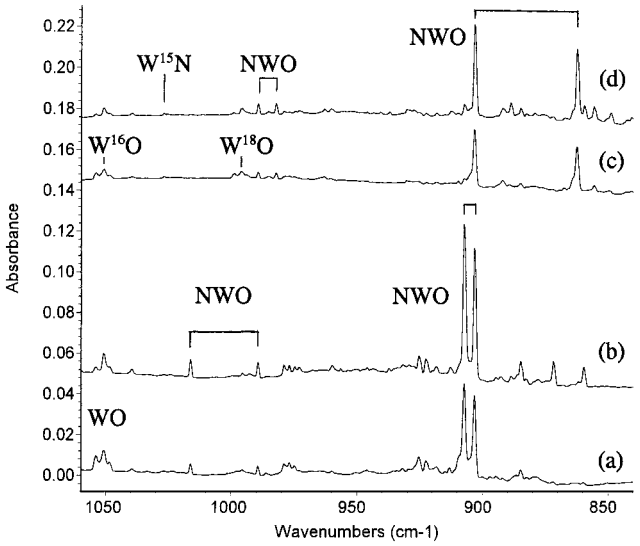

Figure 5. Infrared spectra in the 1060−840 cm^{-1} region for laser-ablated W atoms co-deposited at 10 K with isotopic mixtures in argon: (a) 0.3% (^{14}NO + ^{15}NO) in argon co-deposited for 2 h and (b) after annealing to 25 K; (c) 0.3% (^{15}N^{16}O + ^{15}N^{18}O) in argon co-deposited for 2 h; (d) after annealing to 25 K.

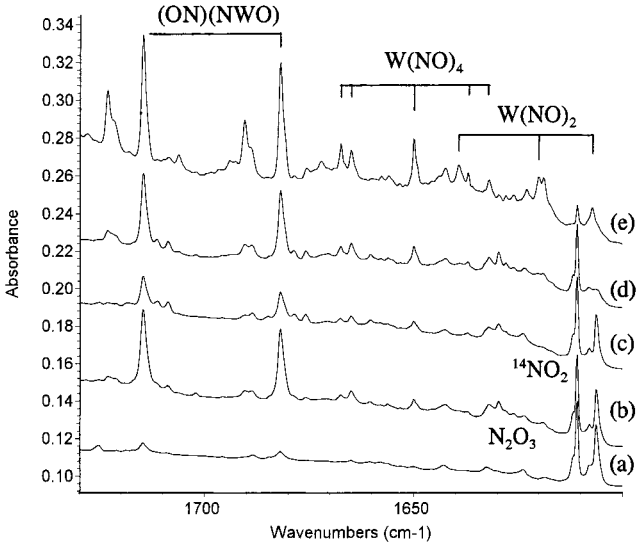

Figure 6. Infrared spectra in the 1730−1600 cm^{-1} region for laser-ablated W atoms co-deposited at 10 K with 0.3% (^{14}NO + ^{15}NO) in argon: (a) sample deposited for 1 h; (b) sample after annealing to 25 K; (c) sample after broad-band photolysis for 30 min; (d) sample after annealing to 30 K; (e) sample after annealing to 40 K.

observed relative band absorbance (1:10) is in reasonable agreement with the (20:91) calculated value. Of more significance is excellent agreement between the calculated and observed normal modes as described by the isotopic shifts. The 1016.3 cm^{-1} band shifts −26.9 cm^{-1} with ^{15}NO and −7.1 cm^{-1} more for ^{15}N^{18}O, and the calculated shifts are −30.0 and −4.8 cm^{-1}; the 907.3 cm^{-1} band shifts −4.1 and −41.0 cm^{-1} with the same reagents, and the calculated shifts are −2.8 and −44.7 cm^{-1}.

Comparison can also be made among NWO (1016, 907 cm^{-1}), WN_2 (870, ν_1 not observed), WO_2 (1025, 978 cm^{-1}), WN (1059.8 cm^{-1}) and WO (1050.9 cm^{-1}).[34,35] Note that the W−N and W−O modes in NWO are slightly lower than for the diatomic molecules and that the average frequency of NWO (962 cm^{-1}) is slightly lower than that for WO_2 (1001 cm^{-1}). Like NMoO, the NWO molecule is both nitride and oxide.

The NMoO and NWO molecules are made by direct insertion reactions 1 and 2 during the deposition process. Excess energy in the ablated atoms, including metastable electronic states,

$$\mathrm{Mo^*} + \mathrm{NO} \rightarrow \mathrm{NMoO} \quad (1)$$

$$\mathrm{W^*} + \mathrm{NO} \rightarrow \mathrm{NWO} \quad (2)$$

makes these reactions favorable. The observation of MoN and WN in these samples suggests that some of the product growth on annealing could be due to the combination of the mononitrides with O atoms. However, the increase for NWO is large enough (almost double on 25 K annealing, Figure 4) to suggest that reaction 2 may also proceed in the cold matrix without activation energy.

MoN and WN. The present experiments gave the same structured band for MoN and almost the same absorption for WN as the analogous experiments with dinitrogen.[35] This is significant in that the absence of excess N_2 makes it unlikely that these MoN and WN species are ligated by dinitrogen.

Complexes Mo-(η^1-NO)$_x$ (x = 1, 2, 3, 4). Following the chromium example, four nitrosyl complexes are expected and the spectra provide evidence for these four complexes.[3] A weak 1620.6 cm^{-1} band increases on annealing, disappears on photolysis, and increases on subsequent annealings while other bands increase even more. The 1620.6 cm^{-1} band shifts to 1586.8 cm^{-1} with ^{15}NO and exhibits a doublet with ^{14}NO + ^{15}NO, indicating the involvement of a single NO molecule (Figure 2). The 14−16/15−16 ratio, 1.021 30, and the 15−16/15−18 ratio, 1.021 24, show substantial departures from the diatomic NO ratios 1.017 94 and 1.027 22, which demonstrate that N is coupled to another atom and is moving more (hence, the larger 14/15 ratio) in this molecule, MoNO, than in diatomic NO itself. Our DFT calculations predict $^4\Sigma^-$ MoNO to be 30.9 kcal/mol above ^{2}A′ NMoO, hence the small yield on sample deposition and growth on annealing, and to have a strong mostly N−O stretching mode at 1691.4 cm^{-1}. Of more importance than agreement with the 1620.6 cm^{-1} experimental band position (0.958 scale factor) are the calculated isotopic frequencies and frequency ratios. The predicted 14−16/15−16 and 15−16/15−18 ratios, 1.021 81 and 1.021 54, are in excellent agreement with the observed ratios, 1.021 30 and 1.021 24. In terms of frequencies, our DFT calculations (scaled) predict Mo^{15}NO and Mo^{15}N^{18}O to be 0.8 cm^{-1} lower and 0.5 cm^{-1} higher than the observed values. This excellent agreement between calculated and observed isotopic frequencies, as a measure of normal vibrational modes, confirms this matrix identification of $^4\Sigma^-$ MoNO.

Another weak band at 1642.7 cm^{-1} grows on annealing, is not affected by photolysis, and grows slightly on higher temperature annealings (Figure 1). The 1642.7 cm^{-1} band shifts to 1611.2 cm^{-1} with ^{15}N^{16}O and to 1572.7 cm^{-1} with ^{15}N^{18}O, giving the ratios 1.019 55 and 1.024 48, which are closer to the diatomic NO values than found for MoNO. Although there is band overlap with the pure isotopic components, a clear, strong 1624.0 cm^{-1} intermediate component is observed with ^{14}NO + ^{15}NO, indicating that *two equivalent* NO submolecules participate in this vibrational mode. Hence, the assignment to Mo-(η^1-NO)$_2$ follows. Note that the strong Cr-(η^1-NO)$_2$ absorption is 14 cm^{-1} higher than Cr-η^1-NO and that 22 cm^{-1} separates the Mo complexes.

The 1656.4 cm^{-1} band and 1653.3 cm^{-1} satellite also show the same annealing and photolysis behavior, and similar isotopic frequency ratios as Mo(NO)$_2$, but these bands show no clear intermediate isotopic absorption. This is consistent with the doubly-degenerate mode of a trigonal trinitrosyl, following the

TABLE 1: Absorptions (cm^{-1}) from Codeposition of Laser-Aablated Mo Atoms with NO in Argon at 10 K

^{14}NO	^{15}NO	^{15}N^{18}O	^{14}NO + ^{15}NO	*R*(14/15)	*R*(16/18)	assignment
2096.0	2026.2	2026.2	2096.0, 2061.5, 2026.2	1.034 45		(N_2) complex
1959.8	1894.8	1894.8	1959.9, 1927.6, 1894.6	1.034 30		(N_2) complex
1872.1	1839.1	1789.5	1872.1, 1839.1	1.017 94	1.027 72	NO
1809.5	1776.4			1.018 63		?
1736.1	1703.6	1661.4	1736.1, 1703.7	1.019 10	1.025 38	(ON)(NMoO)
1730.8	1698.2	1656.5	1730.8, 1698.3	1.019 19	1.025 21	(ON)(NMoO)
1677.5	1646.1	1603.9	1677.4, 1667.3, 1659.3, 1652.3, 1646.0	1.019 08	1.026 31	Mo(NO)$_4$ (T_d)
1667.4	1635.2	1593.7		1.019 69	1.026 04	Mo(NO)$_4$ site
1656.4	1624.1	1585.8	1656.0, 1636.9, 1624.0	1.019 89	1.024 15	(Mo(NO)$_3$)
1642.7	1611.2	1572.7	1642.8, 1624.0, 1611.2	1.019 55	1.024 48	Mo(NO)$_2$
1620.6	1586.8	1553.8	1620.6, 1586.8	1.021 30	1.021 24	Mo(NO)
1576.6	1544.3	1511.0		1.020 92	1.022 04	Mo$_x$(NO)$_y$
1564.1	1532.7	1498.3	1564.1, 1532.7	1.020 49	1.022 96	Mo$_x$(NO)$_y$
1462.5	1437.0	1398.2	1462.5, 1437.0	1.017 72	1.027 72	aggregate
1452.8	1427.5	1389.0	1452.8, 1427.5	1.017 74	1.027 71	aggregate
1427.8	1399.0	1368.1		1.020 59	1.022 59	Mo$_x$(NO)$_y$
1041.4	1011.1	1011.1		1.0299 7		MoN
1037.5	1007.9	1007.8	1037.5, 1007.9	1.029 4		MoN
1002.8	976.1	971.9	1002.8, 976.1	1.027 31	1.004 32	N^{92}MoO
1000.8	974.1	969.8	1000.8, 974.2	1.027 42	1.004 46	N^{95}MoO
1000.2	973.6	969.3	1000.2, 973.6	1.027 35	1.004 44	N^{96}MoO
999.1	972.4	968.0	999.1, 972.4	1.027 43	1.004 49	N^{98}MoO
997.9	971.2	966.8	997.9, 971.2	1.027 49	1.004 54	N^{100}MoO
915	915	874			1.046 9	(MoO_2) complex
891	891	850	891		1.048 2	$^{92}MoO_2$
885	885	845	885		1.047 3	$^{98}MoO_2$
850.9	848.8	811.8	850.9, 848.8	1.002 49	1.045 54	N^{92}MoO
848.5	846.5	809.5		1.002 37	1.045 76	N^{95}MoO
847.9	845.9	808.8		1.002 44	1.045 80	N^{96}MoO
846.5	844.5	807.4	846.5, 844.5	1.002 45	1.045 95	N^{98}MoO
845.2	843.0	805.9	845.2, 843.0	1.002 54	1.046 03	N^{100}MoO
840	838			1.002 4		(ON)(NMoO)
558.0	548.4	543.4		1.017 51	1.009 20	Mo(NO)$_4$ (T_d)
556.3	546.9	541.8		1.017 19	1.009 41	Mo(NO)$_4$ site

TABLE 2: Infrared Absorptions (cm^{-1}) from Codeposition of Laser-Ablated W Atom with NO in Excess Argon at 10 K

^{14}NO	^{15}NO	^{15}N^{18}O	^{14}NO + ^{15}NO	*R*(14/15)	*R*(16/18)	assignment
3643.5	3580.5	3485.5	3643.5, 3612.6, 3580.5	1.017 60	1.027 26	$(NO)_2^+$
3638.0	3575.0	3480.1		1.017 62	1.027 27	$(NO)_2^+$ site
2122.4	2052.2	2052.2	2122.7, 2088.2, 2052.5	1.034 21		N_2 complex
2114.8	2044.7	2044.7	2114.7, 2080.6, 2044.9	1.034 28		N_2 complex
2065.0	1996.3	1996.3	2065.0, 2026.3, 1996.3	1.034 41		N_2 complex
1872.1	1839.1	1789.5	1872.1, 1839.1	1.017 94	1.027 72	NO
1723.3	1690.4	1649.7	1723.4, 1690.5	1.019 46	1.024 67	(ON)(NWO)
1714.9	1681.9	1641.6	1714.8, 1681.9	1.019 62	1.024 55	(ON)(NWO)
1688.5	1660.3			1.016 98		N_2O_3
1667.4	1637.0	1595.0	1667.4, 1649.9, 1637.0	1.018 57	1.026 58	W(NO)$_4$ (C_{2v})
1664.9	1632.0			1.020 16		W(NO)$_4$ (C_{2v})
1655.8	1623.4	1581.6	1656.0, −, 1623.0	1.019 96	1.026 43	(W(NO)$_3$)
1639.2	1607.2		1639.2, 1620.0, 1607.2	1.019 91		W(NO)$_2$
1629.8	1594.0			1.022 46		N_2O_3
1589.3	1562.0	1520.3	1589.3, 1575.2, 1562.0	1.017 48	1.027 43	$(NO)_2^+$
1583.3	1556.2	1514.6	1583.3, 1569.3, 1556.2	1.017 41	1.027 47	$(NO)_2^+$ site
1568.7	1540.0	1501.6		1.018 64	1.025 57	aggregate
1418.2	1393.6		1418.3, 1394.0	1.017 65		aggregate
1407.5	1382.7	1345.2	1407.5, 1383.1	1.017 94	1.027 88	aggregate
1059.8	1026.8	1026.8		1.032 14		WN
1053.9	1053.9	998.9			1.055 06	WO
1050.9	1050.9	996.0			1.055 12	WO
1048.7	1048.7	994.1			1.054 92	WO
1039.7	1039.7	985.0			1.055 53	WO complex
1016.3	989.4	982.3	1016.3, 989.4	1.027 19	1.007 23	NWO
1005.9	979.0			1.027 48		NWO complex
976.9	972.9	927.1	977.0, 972.9	1.004 11	1.049 40	
907.3	903.2	862.2	907.3, 903.1	1.004 54	1.047 55	NWO
893.0	888.8	848.8	892.9, 888.7	1.004 73	1.047 13	NWO complex
885.9	882.5	842.2		1.003 85	1.047 85	NWO complex
883.5	879.4	839.8		1.004 66	1.047 15	NWO complex
871.6	859.4	833.1	871.6, 859.5	1.014 20	1.031 57	(ON)(NWO)
865.4	855.4			1.011 69	1.001 10	?

tricarbonyl example,[36] and the 1656.4 cm^{-1} band is tentatively assigned to Mo-(η^1-NO)$_3$.

The very weak 1677.5 cm^{-1} band increases markedly on first annealing, decreases slightly on photolysis, and increases more markedly on subsequent annealings until it dominates the final annealing spectrum. This band shifts to 1646.1 cm^{-1} with ^{15}N^{16}O and to 1603.9 cm^{-1} with ^{15}N^{18}O, giving isotopic ratios closer still to the diatomic NO values (Table 1). Of more significance is the mixed isotopic spectrum that now shows *three* intermediate mixed isotopic components (Figure 2), which is expected

TABLE 3: Relative Energies and Geometries Calculated for MoNO and WNO Isomer States

molecule	state	relative energy (kcal/mol)	geometry
NMoO	$^2A'$	0	MoN, 1.683 Å; MoO, 1.733 Å; ∠NMoO, 103.7°
MoNO	$^4\Sigma^-$	+30.9	MoN, 1.762 Å; NO, 1.219 Å; ∠MoNO, 180°
Mo[NO]	^4A	+50.4	MoN, 1.853 Å; MoO, 2.012 Å; NO, 1.350 Å
$MoNO^-$	$^3\Sigma^-$	+6.9	MoN, 1.753 Å; NO, 1.246 Å; ∠MoNO, 180°
$MoNO^+$	$^3\Delta$	+214.5	MoN, 1.777 Å; NO, 1.189 Å; ∠MoNO, 180°
NWO	$^2A'$	0	WN, 1.699 Å; WO, 1.727 Å; ∠NWO, 103.6°
WNO	$^4\Sigma^-$	+57.1	WN, 1.756 Å; NO, 1.226 Å; ∠WNO, 180°
W[NO]	^4A	+74.7	WN, 1.827 Å; WO, 1.958 Å; NO, 1.409 Å
WNO^-	$^3\Sigma^-$	+21.1	WN, 1.756 Å; NO, 1.257 Å; ∠WNO, 180°
WNO^+	$^3\Delta$	+253.1	WN, 1.762 Å; NO, 1.185 Å; ∠WNO, 180°

TABLE 4: Isotopic Frequencies (cm^{-1}), Intensities (km/mol), and Ratios of Frequencies Calculated for the Structures Described in Table 3

	14−16	15−16	15−18	*R*(14−16/15−16)	*R*(15−16/15−18)
NMoO	1054.0(44)	1024.5(40)	1022.0(43)	1.0288	1.0024
	907.6(123)	906.3(125)	864.4(112)	1.0014	1.0485
	401.0(1)	394.4(1)	385.3(1)	1.0167	1.0236
MoNO	1691.4(451)	1655.3(436)	1620.4(413)	1.0218	1.0215
	626.6(4)	621.0(4)	602.7(4)	1.0090	1.0304
	348.2(18)	339.3(16)	334.8(17)	1.0262	1.0134
$MoNO^-$	1580.1(806)	1545.1(773)	1514.8(740)	1.0227	1.0200
	628.0(0.1)	622.9(0.2)	603.6(0.1)	1.0082	1.0320
	347.4(0.3)	338.6(0.3)	334.1(0.2)	1.0260	1.0135
$MoNO^+$	1803.1(387)	1766.3(368)	1726.0(356)	1.0208	1.0233
	625.8(0.6)	619.7(0.7)	602.4(0.3)	1.0098	1.0287
	371.6(14)	362.2(13)	357.2(13)	1.0260	1.0140
NWO	1057.0(20)	1027.0(16)	1022.2(20)	1.0292	1.0047
	934.3(91)	931.5(93)	886.8(80)	1.0030	1.0504
	401.6(1)	394.9(1)	385.1(1)	1.0170	1.0254
WNO	1679.6(480)	1642.4(460)	1609.9(440)	1.0226	1.0202
	634.7(1)	628.6(1)	607.4(1)	1.0097	1.0349
	373.7(11)	364.2(10)	359.2(11)	1.0261	1.0139
WNO^-	1557.4(654)	1521.6(629)	1493.8(599)	1.0235	1.0186
	620.6(4)	615.1(3)	593.5(3)	1.0089	1.0364
	352.7(0)	343.6(0)	339.0(0)	1.0265	1.0136
WNO^+	1853.8(422)	1814.5(400)	1775.5(389)	1.0217	1.0220
	647.5(3)	640.6(4)	620.0(3)	1.0108	1.0332
	414.4(9)	403.9(8)	398.2(8)	1.0260	1.0143

for the triply-degenerate mode of a tetrahedral complex.[36] Although the mixed isotopic spectrum for Mo-(η^1-NO)$_4$ is not as clean as the textbook example reported for the 1726.0 cm^{-1} Cr-(η^1-NO)$_4$ band (Figure 5, ref 3), the 1677.5 cm^{-1} band can be assigned with confidence to Mo-(η^1-NO)$_4$. The 48.5 cm^{-1} further red shift in the Mo complex indicates a stronger interaction with NO and suggests that it may be possible to prepare and isolate neat Mo(NO)$_4$.

The weak 558.0 cm^{-1} band shows a contour for the unresolved vibration of natural abundance isotopes for a single Mo atom. The $^{15}N^{16}O$ shift of 10 cm^{-1} and $^{15}N^{18}O$ shift of 5 cm^{-1} more are suggestive of the M−NO vibration, which is also triply degenerate for Mo(NO)$_4$. This weaker mode[3] was observed at 663.0 cm^{-1} for Cr(NO)$_4$, and observation of the Mo(NO)$_4$ counterpart adds more support for the present identification of Mo(NO)$_4$.

(ON)(NMO) Complex. The 1730.8 cm^{-1} band in the Mo system increases markedly on first annealing, decreases substantially on photolysis, and increases slightly on further annealings, much like the final annealing growth of Mo(NO)$_2$. The strong 1730.8 cm^{-1} band shifts with $^{15}N^{16}O$ and $^{15}N^{18}O$ and exhibits a sharp doublet in the mixed isotopic experiment, showing the involvement of one NO submolecule. The 1714.9 cm^{-1} band in the W system shows analogous behavior. In fact, bands at 1747.1 and 1729.6 cm^{-1} in the Nb and Ta systems with NO show analogous behavior as well.[7] These latter bands were assigned to a species (ON)M[NO] with two nonequivalent NO submolecules, one terminal nitrosyl absorbing in the 1700 cm^{-1} region, and one side-bound NO absorbing in the 800 cm^{-1} region. The unique annealing and photolysis behavior of the 1730.8 and 1714.9 cm^{-1} bands allows the association of weaker 838 and 893 cm^{-1} bands with Mo and W, respectively. The observation of major NMoO and NWO primary product bands, and no side-bound M[NO] species, suggests that the present molecules are nitrosyl complexes of the metal oxide−nitride (ON)(NMO).

Complexes W-(η^1-NO)$_x$ (x = 2, 3, 4). The WNO complex is predicted by DFT to absorb at 1679 cm^{-1}, some 12 cm^{-1} below MoNO, but to be 57.1 kcal/mol higher in energy than NWO. Furthermore, the W(NO)$_2$ and W(NO)$_4$ bands to be assigned below are 3 and 10 cm^{-1} below the Mo counterparts. If WNO were formed, it likely would absorb underneath NO_2 at 1611−1606 cm^{-1}. However, the considerably higher energy of WNO argues that this complex may not be trapped because of the much greater stability of the insertion product NWO discussed above.

The weak 1639.2 cm^{-1} band increases on annealing, decreases on photolysis, and increases on further annealing. This band shifts to 1607.2 cm^{-1} with ^{15}NO and gives rise to a triplet with a stronger 1620.0 cm^{-1} intermediate component using ^{14}NO + ^{15}NO, indicating the vibration of two equivalent NO subgroups (Figure 6). Unfortunately the expected position of the $^{15}N^{18}O$ counterpart is masked by strong $^{18}O^{15}N^{16}O$ absorption. The 1639.2 cm^{-1} band is assigned to the antisymmetric N−O stretching mode of W-(η^1-NO)$_2$. This molecule can be made on annealing by reacting W with (NO)$_2$. The 1655.8 cm^{-1} band shows N−O stretching isotopic shifts and similar annealing and photolysis behavior but no intermediate mixed isotopic component. This suggests that the latter is too weak to be observed and is consistent with the degenerate mode of a trigonal W-(η^1-NO)$_3$ complex, as discussed above. Accordingly, the 1655.8 cm^{-1} band is tentatively assigned to W(NO)$_3$.

The sharp 1667.4 and 1664.9 cm^{-1} bands increase on first annealing, decrease slightly on photolysis, and continue increasing *together* on the higher temperature annealings. The bands show $^{15}N^{16}O$ and $^{15}N^{18}O$ isotopic shifts near those for the higher nitrosyls of Cr and Mo. The mixed ^{14}NO + ^{15}NO experiment, however, shows a stronger, sharp 1649.9 cm^{-1} intermediate mixed isotopic band (Figure 6) in contrast to Cr(NO)$_4$ and Mo(NO)$_4$ spectra. In addition, the mixed $^{15}N^{16}O$ + $^{15}N^{18}O$ spectrum also exhibits a stronger, sharp 1612.5 cm^{-1} intermediate mixed isotopic band. This characterizes a vibration involving two equivalent NO subgroups, with the central feature due to vibration of the (ON)W(NO)^i mixed isotopic subunit, probably of C_{2v} symmetry where only pairs of NO subunits couple vibrationally. Furthermore, the observation of *two* bands, 1667.4 and 1664.9 cm^{-1} for the pure isotopic molecule suggests that W-(η^1-NO)$_4$ is distorted. Whether this symmetry reduction from the tetrahedral structure for Cr(NO)$_4$ and Mo(NO)$_4$ is caused by the matrix or is inherent in W(NO)$_4$ itself cannot be determined here. We note that W(CH$_3$)$_6$ and WH$_6$ are lower symmetry (D_{3h}) than might be expected.[37,38]

Other Absorptions. Weak bands at 1576.6, 1564.1, 1452.8, and 1427.8 cm^{-1} increase on annealing, and all but 1452.8 cm^{-1} decrease on photolysis whereas 1452.8 cm^{-1} increases 3 times, and all increase on further annealing. These bands are in the region for Cr(NO)$_x^-$ anion species,[3] but the increase on annealing after decrease on photolysis raises doubts. Mixed ^{14}-NO + ^{15}NO data show that a single NO is involved at 1427.8 cm^{-1}, two NO subunits at 1564.1 cm^{-1}, and the absence of an intermediate component for the 1576.6 cm^{-1} absorption suggests

three or possibly more NO subunits. These bands are probably due to metal cluster nitrosyls most likely with two Mo atoms, but we cannot be certain.

Several other bands in the tables are labeled "complexes". Although the vibrating chromophore is straightforward to identify, the complexing partner is not.

Charged Species. The spectra all contain absorptions for *cis*- and *trans*-$(NO)_2^-$ in agreement with other laser-ablated metal reactions with NO.[27] Furthermore, the bands at 1589.3 and 1583.3 cm^{-1}, which are especially strong in W and Ta experiments,[7] are reaffirmed here to be due to $(NO)_2^+$ in solid argon. These bands form 1/2/1 triplets with mixed $^{14}NO + {}^{15}NO$ (Table 2) and $^{15}N^{16}O + {}^{15}N^{18}O$ (1541.0, 1534.1 cm^{-1} intermediate component), indicating two equivalent NO subgroups. In addition, bands at 3643.5 and 3638.0 cm^{-1} with 4% of the intensity of the 1589.3 and 1583.3 cm^{-1} absorptions track on annealing and photolysis. These bands also form a triplet with mixed isotopes (Table 2) and $^{15}N^{16}O + {}^{15}N^{18}O$ (3534.0 and 3528.7 cm^{-1} intermediate component). The 1589.3 cm^{-1} band is assigned to the ν_5 (b_u) mode and the 3643.5 cm^{-1} band to the ν_1 (a_g) + ν_5 (b_u) combination for *trans*-$(NO)_2^+$. The difference ($3643.5 - 1589.3 = 2054.2$ cm^{-1}) is appropriate for the ν_1 mode in solid argon, after anharmonicity correction. The above bands compare with 3683.9 and 1619.2 cm^{-1} solid neon[24] and 3673 and 1618 cm^{-1} gas-phase ZEKE photoelectron spectra[26] values for $(NO)_2^+$. Note that the 14−16/15−16 frequency ratios for the $\nu_1 + \nu_5$ and ν_5 mode in solid argon, 1.017 60 and 1.017 48, respectively, are essentially the same as the 1.017 62 and 1.017 60 solid neon values.[24] Although changing the neon to the argon matrix red shifts ν_5 from 1619.2 to 1589.3 cm^{-1}, and the combination band from 3683.9 to 3643.5 cm^{-1}, the isotopic ratios (and normal modes) are not changed. How do we provide information on the charged nature of these species? Doping with CCl_4 to serve as an electron trap in Ti + NO experiments[28] *increased* the $(NO)_2^+$ bands by 15% and *decreased* the $(NO)_2^-$ band to 20% of their absorbances without CCl_4. The CCl_4 doping effect confirms the cation and anion identifications.

6. Conclusions

Laser-ablated Mo and W atoms react with NO to give primarily the insertion products NMoO and NWO, but weak MoN and WN absorptions are also observed. The NMoO and NWO molecules are identified from isotopic substitution (^{n}Mo, ^{15}N, ^{18}O) and density functional theory (DFT) calculations. These bent molecules are both nitride and oxide with bonding comparable to the metal dioxide and dinitride molecules. The M−N and M−O frequencies of the $^2A'$ state NMoO and NWO molecules are predicted by DFT (scale factors 0.936 ± 0.004 and 0.966 ± 0.005, respectively), but more importantly, the isotopic shifts (and normal modes) are well-described by DFT frequencies. Furthermore, the calculated bond lengths on going from NMoO to NWO show little change (0.016 Å longer and 0.006 Å shorter), which is a consequence of relativistic contraction between second and third row transition metals compensating for shell expansion.[39] This relativistic effect is also illustrated in the M−N and M−O stretching frequencies for the $^2A'$ NCrO, NMoO, and NWO nitride−oxide molecules, which are 976.1, 999.1, 1016.1 cm^{-1} and 866.2, 846.5, 907.3 cm^{-1}, respectively, in particular by the *increase* on going from NMoO to NWO.

The higher energy MoNO isomer is observed, but WNO and higher energy M-η^2-NO complexes are not found, which is the major difference with the Cr and NO system.[3] The M-$(\eta^1$-NO$)_x$ ($x = 2, 3, 4$) complexes are observed: mixed isotopic splittings indicate that $Mo(NO)_4$ is tetrahedral, like $Cr(NO)_4$, but the spectra show that $W(NO)_4$ is distorted to C_{2v} symmetry.

Finally, the large yield of charged species in these experiments made possible observation of a weak 3643.5 cm^{-1} combination band in addition to the strong 1589.3 cm^{-1} fundamental for $(NO)_2^+$ and the strong 1222.8 and 1221.0 cm^{-1} fundamentals for *cis*- and *trans*-$(NO)_2^-$.

Acknowledgment. We gratefully acknowledge NSF support under Grant CHE 97-00116.

References and Notes

(1) Castleman, A. W., Jr.; Bowen, K. H., Jr. *J. Phys. Chem.* **1996**, *100*, 12911.
(2) Bacic, Z.; Miller, R. E. *J. Phys. Chem.* **1996**, *100*, 12945.
(3) Zhou, M. F.; Andrews, L. *J. Phys. Chem. A* **1998**, *102*, 7452.
(4) Chertihin, G. V.; Bare, W. D.; Andrews, L. *J. Chem. Phys.* **1997**, *107*, 2798.
(5) Andrews, L.; Bare, W. D.; Chertihin, G. V. *J. Phys. Chem. A* **1997**, *101*, 8417.
(6) Zhou, M. F.; Andrews, L. *J. Phys. Chem. A* **1999**, *103*, 478.
(7) Zhou, M. F.; Andrews, L. *J. Phys. Chem. A* **1998**, *102*, 10025.
(8) Herberhold, M.; Razasi, A. *Angew. Chem., Int. Ed. Engl.* **1972**, *11*, 1092.
(9) Swanson, B. I.; Satija, S. K. *J. Chem. Soc., Chem. Commun.* **1973**, 40.
(10) Huber, K. J.; Aita, C. R. *J. Vac. Sci. Technol. A* **1988**, *6*, 1717.
(11) Porowski, S.; Grzegory, I.; Morawski, A. *Mater. Processes* **1992**, *3*, 227.
(12) Bechinger, C.; Oefinger, G.; Herminghaus, S. *J. Appl. Phys.* **1993**, *74*, 4527.
(13) Ho, K. C.; Rukavina, T. G.; Greenberg, C. B. *J. Electrochem. Soc.* **1994**, *141*, 2061.
(14) Kim, Y.-T.; Lee, C.-W. *J. Appl. Phys.* **1994**, *76*, 542.
(15) Ramanathan, S.; Oyama, S.-T. *J. Phys. Chem.* **1995**, *99*, 16365.
(16) Meijers, S.; Gielgens, L. H.; Ponec, V. *J. Catal.* **1995**, *156*, 147.
(17) Conte, V. Difuria, F.; Moro, S. *J. Phys. Org. Chem.* **1996**, *9*, 329.
(18) Batchelor, R. A.; Burdis, M. S.; Siddle, J. R. *J. Electrochem. Soc.* **1996**, *143*, 1050.
(19) Williams, W. S. *J. Met.* **1997**, *49*, 38.
(20) Matsuda, T.; Sakagami, H.; Takahashi, N. *J. Chem. Soc., Faraday Trans.* **1997**, *93*, 2225.
(21) Burkholder, T. R.; Andrews, L. *J. Chem. Phys.* **1991**, *95*, 8697.
(22) Hassanzadeh, P.; Andrews, L. *J. Phys. Chem.* **1992**, *96*, 9177.
(23) Milligan, D. E.; Jacox, M. E. *J. Chem. Phys.* **1971**, *55*, 3404.
(24) Jacox, M. E.; Thompson, W. E. *J. Chem. Phys.* **1990**, *93*, 7609.
(25) Hacaloglu, J.; Suzer, S.; Andrews, L. *J. Phys. Chem.* **1990**, *94*, 1759.
(26) Strobel, A.; Knoblauch, N.; Agreiter, J.; Smith, A. M.; Nerder-Schatteburg, G.; Bondybey, V. E. *J. Phys. Chem.* **1995**, *99*, 872
(27) Andrews, L.; Zhou, M. F.; Willson, S. P.; Kushto, G. P.; Snis, A.; Panas, I. *J. Chem. Phys.* **1998**, *109*, 177.
(28) Kushto, G. P.; Zhou, M. F.; Andrews, L. *J. Phys. Chem. A* **1999**, *103*, 1115.
(29) Frisch, M. J.; Trucks, G. W.; Schlegel, H. B.; Gill, P. M. W.; Johnson, B. G.; Robb, M. A.; Cheeseman, J. R.; Keith, T.; Petersson, G. A.; Montgomery, J. A.; Raghavachari, K.; Al-Laham, M. A.; Zakrzewski, V. G.; Ortiz, J. V.; Foresman, J. B.; Cioslowski, J.; Stefanov, B. B.; Nanayakkara, A.; Challacombe, M.; Peng, C. Y.; Ayala, P. Y.; Chen, W.; Wong, M. W.; Andres, J. L.; Replogle, E. S.; Gomperts, R.; Martin, R. L.; Fox, D. J.; Binkley, J. S.; Defrees, D. J.; Baker, J.; Stewart, J. P.; Head-Gordon, M.; Gonzalez, C.; Pople, J. A. *Gaussian 94, Revision B.1*; Gaussian, Inc.: Pittsburgh, PA, 1995.
(30) Perdew, J. P. *Phys. Rev. B* **1986**, *33*, 8822. Becke, A. D. *J. Chem. Phys.* **1993**, *98*, 5648.
(31) Dunning, T. H., Jr.; Hay, P. J. in *Modern Theoretical Chemistry*; Schaefer, H. F., III, Ed.; Plenum: NewYork, 1976.
(32) Hay, P. J.; Wadt, W. R. *J. Chem. Phys.* **1985**, *82*, 299.
(33) Bytheway, I.; Wong, M. W. *Chem. Phys. Lett.* **1998**, *282*, 219.
(34) Bare, W. D.; Souter, P. F.; Andrews, L. *J. Phys. Chem. A* **1998**, *102*, 8279. Zhou, M. F.; Andrews, L. To be published.
(35) Andrews, L.; Souter, P. F.; Bare, W. D.; Liang, B. *J. Phys. Chem. A*, in press.
(36) Darling, J. H.; Ogden, J. S. *J. Chem. Soc., Dalton Trans.* **1972**, 2496.
(37) Haaland, A.; Hammel, A.; Rypdal, K.; Volden, H. V. *J. Am. Chem. Soc.* **1990**, *112*, 4547.
(38) Kaupp, M. *J. Am. Chem. Soc.* **1996**, *118*, 3018.
(39) Pyykko, P. *Chem. Rev.* **1988**, *88*, 563.